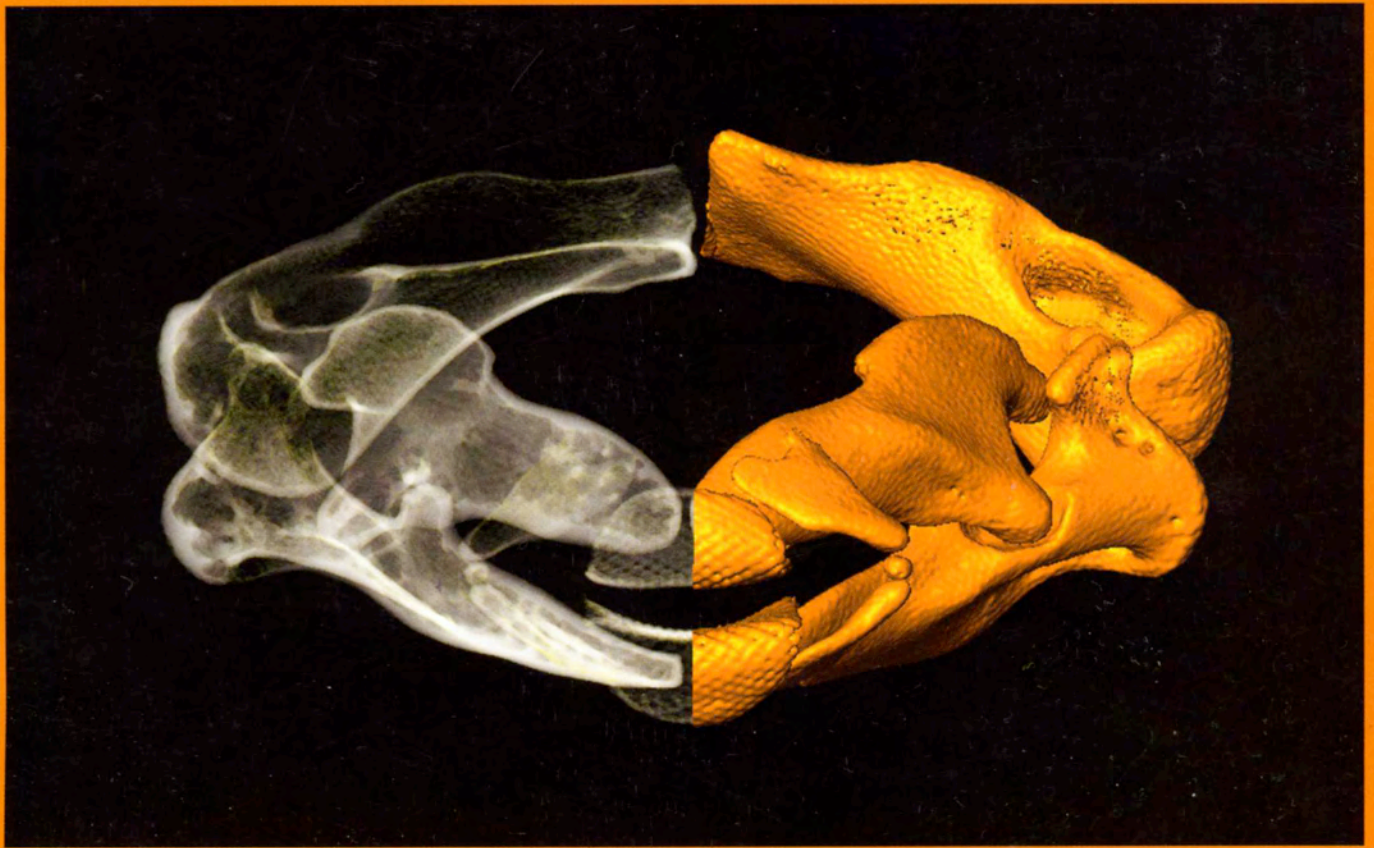


Volume 267 Number 10 October 2006

JOURNAL OF

morphology

ISSN 0362-2525



Editor

FREDERICK W. HARRISON

 WILEY-LISS

Discover papers in this journal online, ahead of the print issue, through EarlyView®
 WILEY
InferScience®
DISCOVER SOMETHING GREAT
www.interscience.wiley.com

Functional Morphology of Jaw Trabeculation in the Lesser Electric Ray *Narcine brasiliensis*, With Comments on the Evolution of Structural Support in the Batoidea

Mason N. Dean,^{1*} Daniel R. Huber,² and Holly A. Nance³

¹*Ecology and Evolutionary Biology, University of California Irvine, Irvine, California 92697-2525*

²*Department of Biology, University of South Florida, Tampa, Florida 33620*

³*Department of Marine Sciences, The University of North Carolina, Chapel Hill, North Carolina 27599-3300*

ABSTRACT The design of minimum-weight structures that retain their integrity under dynamic loading regimes has long challenged engineers. One solution to this problem found in both human and biological design is the optimization of weight and strength by hollowing a structure and replacing its inner core with supportive struts. In animals, this design is observed in sand dollar test, avian beak, and the cancellous bone of tetrapod limbs. Additionally, within the elasmobranch fishes, mineralized trabeculae (struts) have been reported in the jaws of durophagous myliobatid stingrays (Elasmobranchii: Batoidea), but were believed to be absent in basal members of the batoid clade. This study, however, presents an additional case of batoid trabeculation in the lesser electric ray, *Narcine brasiliensis* (Torpediniformes). The trabeculae in these species likely play different functional roles. Stingrays use their reinforced jaws to crush bivalves, yet *N. brasiliensis* feeds by ballistically protruding its jaws into the sediment to capture polychaetes. In *N. brasiliensis*, trabeculae are localized to areas likely to experience the highest load: the quadratomandibular jaw joints, hyomandibular-cranial joint, and the thinnest sections of the jaws immediately lateral to the symphyses. However, the supports perform different functions dependent on location. In regions where the jaws are loaded transversely (as in durophagous rays), “load leading” trabeculae distribute compressive forces from the cortex through the lumen of the jaws. In the parasymphyseal regions of the jaws, “truss” trabeculae form cross-braces perpendicular to the long axes of the jaws. At peak protrusion, the jaw arch is medially compressed and the jaw loaded axially such that these trabeculae are positioned to resist buckling associated with excavation forces. “Truss” trabeculae function to maintain the second moment of area in the thinnest regions of the jaws, illustrating a novel function for batoid trabeculation. Thus, this method of structural support appears to have arisen twice independently in batoids and performs strikingly different ecological functions associated with the distribution of extreme loading environments. *J. Morphol.* 267: 1137–1146, 2006. © 2004 Wiley-Liss, Inc.

KEY WORDS: trabeculae; elasmobranch; biomechanics; Euler buckling; CT scan

Predation is mechanically demanding: in order to avoid structural damage to the skeleton, dynamic loads such as those associated with feeding must be received and managed (Wainwright et al., 1976; Seilacher, 1979b). However, robust skeletons often sacrifice reduced weight for resistance to high loads. In a trade-off between strength and economy of materials, the ideal design is one where the maximum load can be received and dissipated with a structure of minimum weight (i.e., strength/unit weight is maximized) (Wainwright et al., 1976; Lanyon and Rubin, 1985; Hylander and Johnson, 1997).

Material is needed only in those areas that experience the most strenuous loads. An economical structural solution can therefore be reached by arranging tissue along lines of principle stress (Currey, 1984). In this way, the internal architecture of skeletal elements maps regular loading patterns of intrinsic compression and tension, a relationship between form and mechanical loading known as “Wolff’s Law” (Lanyon and Rubin, 1985; Martin et al., 1998; Swartz et al., 1998). For example, in the ends (diaphyses) of mammalian long bones, struts known as trabeculae span the lumen to transmit articular forces and buttress the cortex (Currey, 2002). Analogs to mammalian trabeculae are found resisting and redistributing compressive forces in echinoid test, cuttlebone, hedgehog spines, porcupine quills, and avian limbs and skulls (Bock, 1964,

Supplementary material for this article is available via the Internet at <http://www.interscience.wiley.com/jpages/0362-2525/suppmat>

Contract grant sponsor: AES Nelson Behavioral Research Award (to M.D.).

*Correspondence to: Mason Dean, Ecology and Evolutionary Biology, University of California, 321 Steinhaus Hall, Irvine, CA 92697-2525. E-mail: mdean@uci.edu

Published online 9 December 2004 in
Wiley InterScience (www.interscience.wiley.com)
DOI: 10.1002/jmor.10302

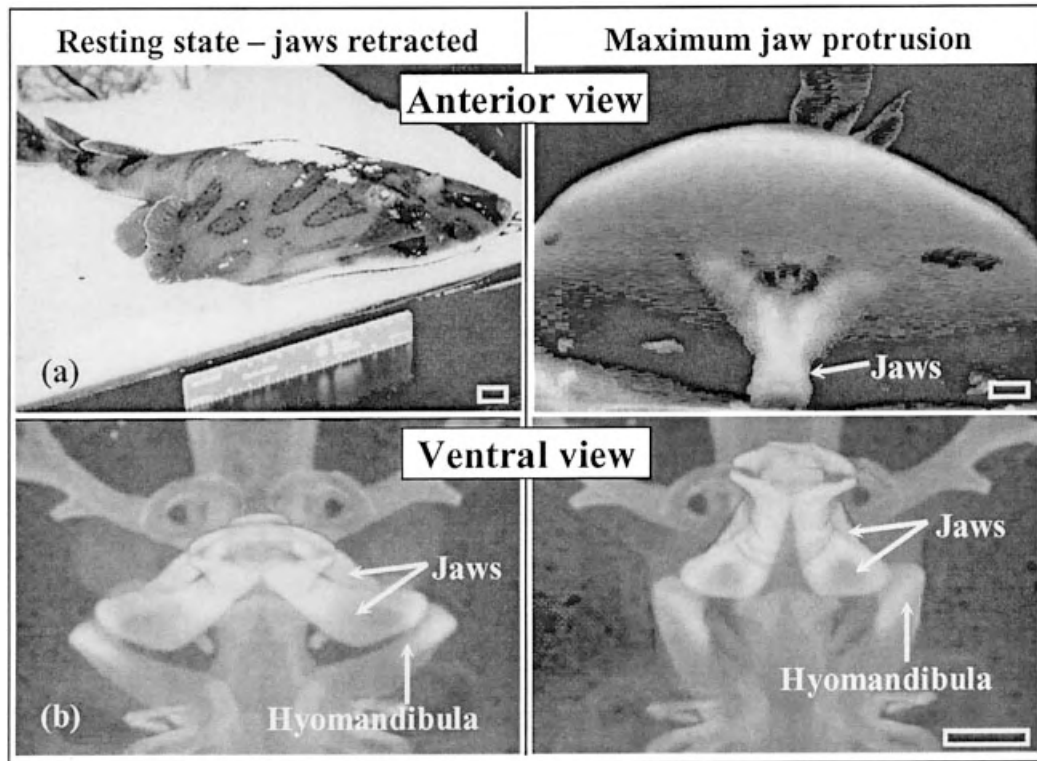


Fig. 1. Jaw protrusion kinematics and mechanics in *Narcine brasiliensis*. This species (a, left column; in right anterolateral view) is capable of extreme jaw protrusion (a, right column; in anterior view taken from high-speed video, 500 fps) for excavation of buried prey. Protrusion is nearly 100% of head length and is accomplished through medial compression of the jaw arch, resulting in part from hyomandibular rotation (b, images are ventral CT scans of a 14.5 cm disk width female with anterior toward the top of the page). The hyomandibula supports the distal edge of the lower jaw (Meckel's cartilage), which is morphologically coupled with the upper jaw (palatoquadrate) such that the jaw arch protrudes as an "oral tube." Scale bars = 1 cm.

1968; Seilacher, 1979a; Vincent and Owers, 1986; Sherrard, 2000). Tissue arrangement can be simplified by localizing the highest stresses and making force trajectories more consistent, either through the animal's behavior or the mechanical design of the skeletal element.

In cartilaginous fishes, trabeculation was previously believed to be present only in the jaws of myliobatid stingrays. Trabeculae extend from the occlusal surface to the opposite face of the jaws, thereby connecting the dorsal and ventral surfaces of the cortex (Summers et al., 1998; Summers, 2000). The arrangement of trabeculae normal to the tooth plates resists the compressive forces associated with durophagy, where the prey may be harder than the cartilaginous jaws themselves. Trabeculae are also retained in the derived planktivorous myliobatid *Manta* species.

We have found structurally similar struts in the jaws of the lesser electric ray, *Narcine brasiliensis*. This species is an inertial suction feeder, exhibiting strikingly different prey capture behavior to myliobatid stingrays. *Narcine brasiliensis* possesses a unique and dynamic jaw protrusion mechanism in which the jaws are extended 100% of head length and shoved beneath the sand to capture benthic

polychaetes (Fig. 1; Dean and Motta, 2004b). Once the prey item is grasped, the jaws are repeatedly protruded and retracted, creating internal pressure oscillations to winnow the food from ingested sediment.

Although the jaws have a wide range of motion once protruded, the palatoquadrate (upper jaw) and Meckel's cartilage (lower jaw) are morphologically coupled by dual quadratomandibular joints and overlapping cartilaginous processes (Fig. 2). As a result, the palatoquadrate and Meckel's cartilage are constrained to extend as a unit (Fig. 1). Protrusion is accomplished via medioventral rotation of the paired hyomandibular cartilages, which are the sole means of suspension of the jaw arch from the cranium. This rotation translates into medial folding of the jaw arch, reducing the symphyseal angle and projecting the jaws. Although the hyomandibular-mandibular joint and the jaw symphyses are freely mobile, motion of the palatoquadrate and Meckel's cartilage relative to one another is largely restricted to the sagittal plane (opening and closing of the jaws).

The cortex of elasmobranch jaw cartilage comprises one or several layers of discrete mineralized blocks known as tesserae. These calcified blocks

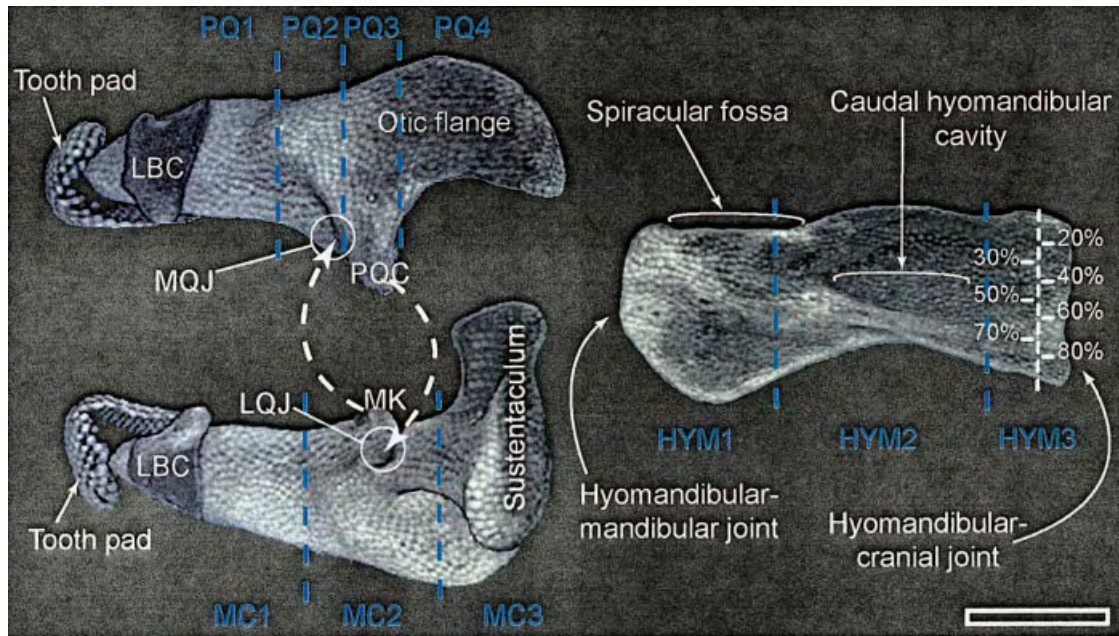


Fig. 2. Divisions for assessment of calcification in the palatoquadrate, Meckel's cartilage, and hyomandibula of *Narcine brasiliensis* (male, 18.2 cm disk width; anterior to the left). Each element was divided longitudinally into 3–4 segments (e.g., PQ1, PQ2) based on anatomical landmarks and functional units. The internal calcification of each segment was investigated from cutaway CT scans at depths of 20–80% (moving dorsoventrally) in 10% increments (e.g., as illustrated for segment HYM3). HYM, hyomandibula; LBC, labial cartilage; LQJ, lateral quadratomandibular joint; MC, Meckel's cartilage; MK, mandibular knob; MQJ, medial quadratomandibular joint; PQ, palatoquadrate; PQC, palatoquadrate condyle. Scale bar = 1 cm.

overlie the uncalcified hyaline cartilage that fills the lumen (Moss, 1977; Dingerkus et al., 1991a). Therefore, elasmobranch skeletal elements can be reinforced in two ways: through thickening of the cortex and/or addition of trabeculae.

The consistent and specific nature of protrusion mechanics in *Narcine brasiliensis* and its invertebrate diet (primarily polychaetes) suggest a loading regime and resultant tissue arrangement entirely different from stingrays. The purpose of this study was to describe the distribution of calcified cartilage (trabeculae and cortical thickening) in the jaws of *N. brasiliensis*. Assuming Wolff's Law, this architecture could then be used to make inferences regarding the forces experienced by the jaws in this unique ballistic feeding mechanism. Trabeculation in *N. brasiliensis* could also be compared with myliobatid stingray trabeculation (Summers, 2000) to address the biological role of jaw reinforcement design in the two groups and hypothesize the evolutionary pathway of trabeculation in batoid fishes.

MATERIALS AND METHODS

Computed Tomography

The jaws of four specimens (males: juvenile 9.1 cm, adult 18.2 cm DW; juvenile 9.9 cm, adult 17.3 cm DW; supplied by the Florida Museum of Natural History, Gainesville, FL #UF 124508) of *Narcine brasiliensis* were scanned at The University of Texas High-Resolution X-Ray Computed Tomography Facility. Computed tomography (CT) provides a nondestructive means to im-

age the interiors of opaque objects in three dimensions (Ketcham and Carlson, 2001; Summers et al., 2004). The technique relies on the differential attenuation of X-rays as they pass through materials of varying density and composition (such as calcified compared to noncalcified cartilaginous tissues in Chondrichthyes) to generate a series of digital "slices" in which grayscale values correspond to density and elemental contrast. This technology provides a powerful tool for the morphologist that transcends the benefits of conventional radiography in that objects can be rotated and sectioned virtually in any plane.

Because of their different sizes, separate scanning protocols were employed for the adult and juvenile rays. Scans of adult rays were reconstructed using a 51.4 mm field of view on 1024×1024 pixel images with a slice thickness and interslice spacing of 0.0536 mm. Scans of juvenile rays were reconstructed using a 37.0 mm field of view on 1024×1024 pixel images with a slice thickness and interslice spacing of 0.0449 mm.

The series of CT slices was rendered as three-dimensional (3D) visualizations to illustrate the external morphology of the jaws and the locations of internal structures such as trabeculae. In order to image process these data, the original 16-bit scanned images were lowered to 8 bit in Adobe PhotoShop 6.0 (Adobe Systems, San Jose, CA), and the two adult specimens were downsized from 1024×1024 pixel to 768×768 pixel images. VoxBlast (VayTek, Fairfield, IA) was used to render 3D images of the jaws, which were subsequently animated using Quicktime Pro 5.0 (Apple Computer). These animations included four movies for each specimen: two cut-away movies, one digitally slicing through the horizontal plane, and one slicing through the sagittal plane, and two movies in which the specimens were rotated about their vertical and horizontal axes, respectively. The cut-away movies were used to investigate calcification patterns of the cranial elements, while movies rotating the specimens about their horizontal and vertical axes were used for gross morphological descriptions.

Morphological Analysis

Trabeculation and tesseration patterns were examined for the left palatoquadrate, Meckel's cartilage, and hyomandibula of each specimen. The mechanical function of the calcified structures could then be proposed based on the regions of high cortical thickness, the location and orientation of trabeculae, and kinematic and behavioral observations of jaw use in live, captive animals (Dean and Motta, 2004b).

To investigate distribution of calcification within the three skeletal elements, each structure was subdivided into a series of units (e.g., PQ1, PQ2; Fig. 2) chosen by their morphological distinctness and identifiable by clear anatomical landmarks. These divisions isolate functional units and points of interaction between skeletal elements, as determined from previous anatomical and behavioral studies of this species (Dean and Motta, 2004a, b).

The palatoquadrate was divided into four segments: symphysis to the anterior edge of the otic flange (PQ1); anterior edge of the otic flange to posterior margin of the medial quadratomandibular joint (where the mandibular knob articulates with the palatoquadrate) (PQ2); posterior edge of the medial quadratomandibular joint to the posterior margin of the palatoquadrate condyle (PQ3); posterior margin of the palatoquadrate condyle to the end of the otic flange (PQ4).

Meckel's cartilage was divided into three segments: symphysis to the anterior edge of the mandibular knob (MC1); anterior edge of the mandibular knob to the anterior edge of the sustentaculum (MC2); and anterior edge of the sustentaculum to the end of the sustentaculum (MC3). Lastly, the hyomandibula was divided into three segments: distal articular surface of the hyomandibula to the medial edge of the spiracular fossa (HYM1); medial edge of the dorsal hyomandibular fossa to the medial edge of the caudal hyomandibular concavity (HYM2); and medial edge of the caudal hyomandibular concavity to the proximal end of the hyomandibula (HYM3).

The first segments in the palatoquadrate and Meckel's cartilage (PQ1, MC1) correspond to the parasymphyseal regions of the jaw (adjacent to the symphyses), while the second segments (PQ2, MC2) delimit the medial quadratomandibular joint and PQ3 and MC2 include the lateral quadratomandibular joint. The remaining sections of the upper and lower jaws (PQ4, MC3) comprise those portions caudal to the lateral joint. The hyomandibula is divided into its mandibular articulation (HYM1), medial portion (HYM2), and cranial articulation (HYM3).

Calcification was analyzed at varying depths within the divisions of each element, using horizontal cut-away videos. Motion-scope 2.01 software (Redlake MASD, San Diego, CA) was used to isolate frames corresponding to depths of 20%, 30%, 40%, 50%, 60%, 70%, and 80% (e.g., Fig. 2, HYM3) moving from the dorsal to ventral faces through each segment of the palatoquadrate, Meckel's cartilage, and hyomandibula. At each depth in every segment (e.g., 20% depth, PQ1) the cross-sectional area was measured and number of trabeculae counted. Both types of calcification (trabeculation and tesseration/cortical thickening) were then calculated as a percentage of cross-sectional area using SigmaScan Pro 4.01 image analysis software (SPSS, Chicago, IL).

These data illustrate the relative contribution of each type of calcification to overall mineralization. The small sample size precluded statistical analyses; however, trabecular placement was extremely consistent among individuals (see Results section). Data are therefore presented, for each segment depth, as average percent cross-sectional area occupied by each type of mineralization.

RESULTS

Trabeculation

Trabeculae were localized to specific regions in all skeletal elements examined (Figs. 3, 4). These "trabecular groups" were always found in the same segment (e.g., PQ1), yet exhibited some intraindividual

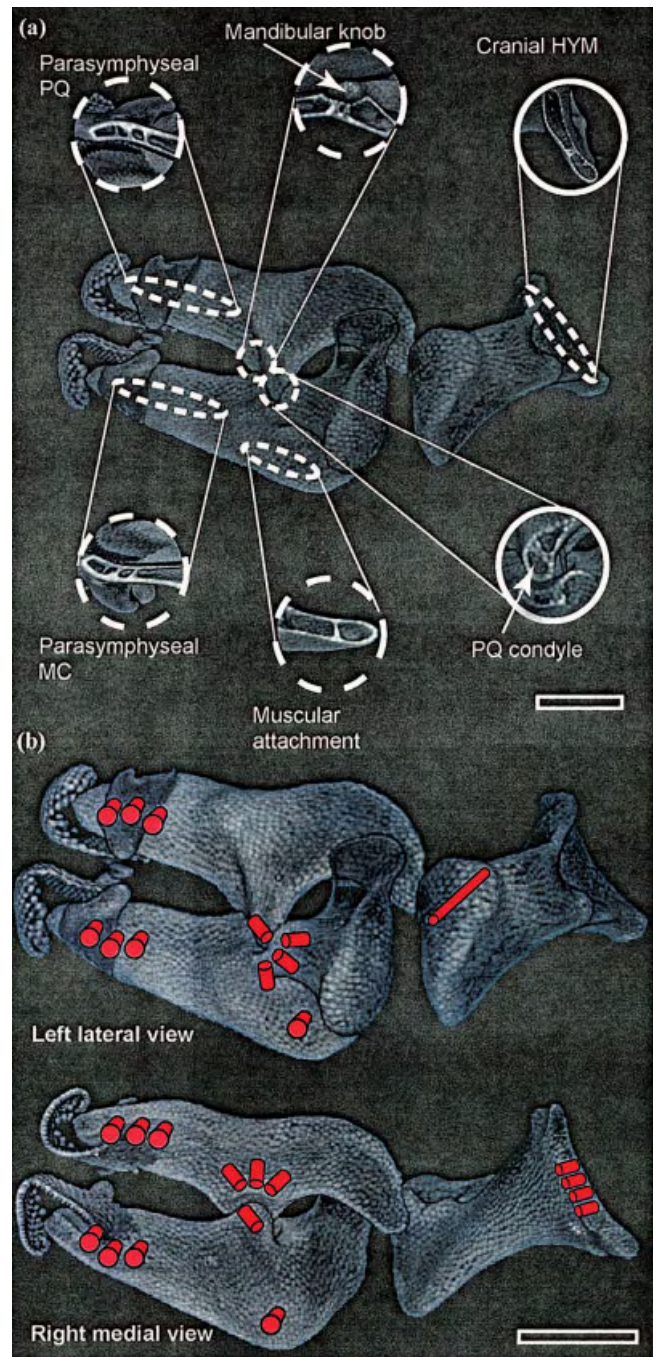


Fig. 3. Localization of trabeculation in the jaws and hyomandibula of *Narcine brasiliensis*; trabeculae are found consistently in the same regions (a). Expanded white circles illustrate trabeculation within a given area with text indicating relevant regional landmarks. Solid circles present elements in lateral view (the same orientation as the larger image of the jaws and hyomandibula), while dashed circles provide a dorsal view. The orientation of trabeculation groups is shown schematically (b) in left lateral (top) and right lingual (bottom) views, with trabeculae represented as columns. HYM, hyomandibula; MC, Meckel's cartilage; PQ, palatoquadrate. Scale bars = 1 cm.

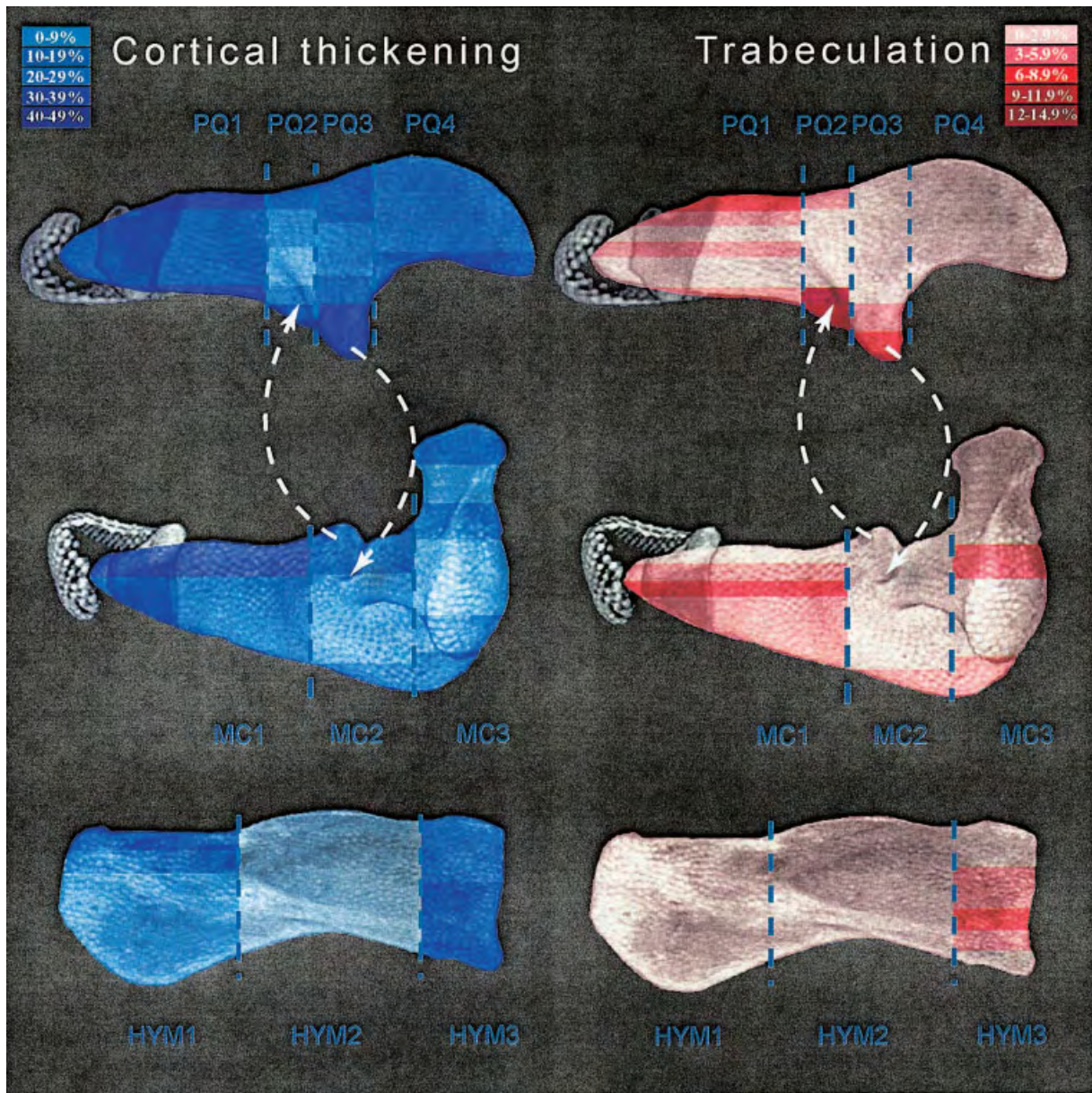


Fig. 4. Cortical thickness and trabeculation in the jaws and hyomandibula of *Narcine brasiliensis*. Anterior is to the left. Skeletal elements are divided into 3–4 longitudinal segments (turquoise lines and text) and data are represented as percent area occupied at varying dorsal–ventral depths provided by CT scan cutaway videos. Color scales are presented at the top, with darker colors representing a higher percentage contribution of cortex or trabeculae. White arrows indicate articulations for medial (upward arrow) and lateral (downward arrow) quadratomandibular joints. Note that most areas of dense trabeculation correspond to areas of thickened cortex. Scale bar = 1 cm.

variation in the depth at which they were found in each element (Table 1). The orientation of trabeculae in these regions was also consistent (Fig. 3). These observations were supported by dissections of the jaws and hyomandibulae (Dean, unpubl. data).

The parasymphyseal regions of the palatoquadrate and Meckel's cartilage were characterized by comparatively extensive trabeculation, extending from the lateral face of the jaw element to its medial surface. The parasymphyseal trabeculae are thus

oriented perpendicular to the longitudinal axes of each jaw ramus (Fig. 3).

The medial and lateral quadratomandibular joints contain trabeculae in the fossae and condyles of both joints. Trabeculation spans the minor axis of the condyles, perpendicular to the longitudinal axes of the condylar processes. The fossae, however, exhibited trabeculation that radiates in multiple directions from the articular surfaces that receive the condyles. In other words, radial trabeculation was

TABLE 1. Depth variation of trabecular groupings in the jaw arch and hyomandibulae of *Narcine brasiliensis* (n = 4)

Trabecular group	Segment	Mean depth \pm SD	Mean %CSA \pm SD
Parasymphyseal	PQ1	38.80 \pm 11.52	7.64 \pm 4.26
	MC1	52.85 \pm 17.52	9.25 \pm 4.87
Medial quadratomandibular joint	PQ2	65.00 \pm 11.39	15.91 \pm 7.86
	MC2	53.75 \pm 18.87	5.87 \pm 2.61
Lateral quadratomandibular joint	PQ3	77.5 \pm 3.54	12.99 \pm 2.40
	MC2	53.75 \pm 18.87	5.87 \pm 2.61
Depressor mandibularis insertion	MC3	58.75 \pm 4.79	6.79 \pm 3.14
Hyomandibular-mandibular joint	HYM1	52.5 \pm 10.61	4.03 \pm 1.08
Craniohyomandibular joint	HYM3	61.67 \pm 8.82	11.03 \pm 4.23

Trabeculation is localized to specific regions of the jaws and hyomandibulae and therefore shows little variation in location. Depth of each grouping is represented as a percentage of distance from the dorsal to the ventral surfaces of each skeletal element, plus or minus standard deviation. The mean percent cross-sectional area occupied by each trabecular group is presented in the last column. HYM, hyomandibula; MC, Meckel's cartilage; PQ, palatoquadrate.

contained in the Meckel's cartilage beneath the fossa receiving the palatoquadrate condyle (lateral quadratomandibular joint) and the palatoquadrate exhibited radial trabeculation about its articulation with the mandibular knob (medial quadratomandibular joint). These quadratomandibular trabeculae therefore reinforce the plane of rotation of the joints (sagittal opening and closing) (Fig. 3).

In all specimens a single trabecula is located ventral to the jaw joints in Meckel's cartilage near the insertion of the depressor mandibularis muscle, which likely aids in adduction of halves of the lower jaw during jaw protrusion (Dean and Motta, 2004a, b). This trabecula extends from the lateral to the medial face of Meckel's cartilage.

Lastly, trabeculae were found in both articular regions of the hyomandibulae. These trabeculae are oriented perpendicular to the long-axis of the hyomandibula, where it articulates with Meckel's cartilage and the cranium. The hyomandibulae is rectangular and compressiform at these articulations, with the trabeculae spanning the minor axis of the element at both articulations. Trabeculae at the hyomandibular-mandibular articulation were only found in two specimens (adult male, juvenile female) and contributed less than 5% of cross-sectional area in the slices in which they were found and therefore are not visible in Figure 4 (Table 1).

Cortical Thickening

Cortical thickening always occupied a larger percent of cross-sectional area ($26.59 \pm 12.19\%$, maximum = 54.46%) than trabeculation ($8.66 \pm 4.01\%$, maximum = 19.51%) in areas of co-occurrence. Cortical thickening in the jaws is greatest at the dorsal and ventral margins of both jaw elements and in the articulating surfaces of the quadratomandibular joints (Figs. 3, 4). In the hyomandibula, the cortex

is thickest at the distal dorsal surface (hyomandibular-mandibular articulation) and the element's proximal articulation with the cranium. The placement of trabeculation mirrored the majority of regions of high cortical thickness (i.e., parasymphyseal regions, quadratomandibular joints, cranio-hyomandibular joint).

The cortex is notably thinner in the medial portions (approximate center of mass) of all skeletal elements. The medial portion of the hyomandibula, in particular, was partially transparent in CT scans and in fresh specimens could be freely twisted about the element's long axis (Figs. 3, 4).

The placement of trabeculation either has no relation to cortical thickness (i.e., often, regions of thick and thin cortex both lacked trabeculae) or mirrors the regions of high cortical thickness (i.e., parasymphyseal regions, quadratomandibular joints, cranio-hyomandibular joint) (Fig. 4). This variation in the interaction of the two types of mineralization was often found in a single segment (e.g., PQ1), creating localized patches of trabeculae.

DISCUSSION

Restricted or consistent patterns of loading are typically resisted by anisotropic architecture, with supporting material distributed along lines of stress (Wainwright et al., 1976; Thomason, 1995; Shiller et al., 2002). The consistent placement of trabecular groups (Fig. 3) is likely due to the restricted loading patterns associated with the morphologically constrained protrusion mechanism of *Narcine brasiliensis* (Dean and Motta, 2004a, b).

The parasymphyseal trabeculation in both the palatoquadrate and Meckel's cartilage is perpendicular to the long axis of the jaws, and therefore normal to the forces associated with excavation of prey. At peak protrusion, the long-axes of the two halves

of the jaws are nearly parallel, forming an oral tube oriented perpendicular to the sediment (Dean and Motta, 2004a, b). Parasymphyseal trabeculae would therefore act as cross-braces (Currey, 1984; Vincent and Owers, 1986), spanning the lumen to brace the cortex against lateral movement and prevent excessive deflection and failure (Euler buckling).

Trabeculation in the jaw joints likely serves two purposes: bracing the articular surfaces of the jaws during opening and closing, and resisting joint compression during excavation. The radial orientation of these trabeculae will resist the joint reaction forces of the lateral and medial quadratomandibular joints throughout a range of gape and symphyseal angles. This is desirable for a rotating system subject to ballistic movements because joint reaction forces can be of roughly the same magnitude as the forces responsible for jaw kinesis (Herrel et al., 1998; Martin et al., 1998). This is especially relevant for the prey-processing behavior of *Narcine brasiliensis*, in which the jaws are repeatedly protruded and retracted to expel sediment from the buccal cavity (Dean and Motta, 2004b). Excavation of buried prey exerts a compressive force directed along the longitudinal axis of the protruded jaws as well. The plane of articulation of the quadratomandibular joints is perpendicular to this vector, thus necessitating reinforcement.

The single trabecula at the base of each half of Meckel's cartilage is apparently associated with the depressor mandibularis muscle, which aids in medially compressing the jaws for protrusion. This point on Meckel's cartilage likely experiences high stresses, as heterotopic elements (cartilaginous nodules) were found beneath the depressor mandibularis tendon, wrapping around the ventral margin of Meckel's cartilage (Olson, 2000; Dean and Motta, 2004a). The heterotopic element likely acts as a jib, increasing the lever arm of force in the depressor mandibularis system (as in the rectus femoris tendon coursing over the human patella; Currey, 2002), with the single trabecula helping to resist the regionally restricted loading.

Hyomandibular trabeculae were found at both the mandibular and the cranial articulations. These struts span the minor axis of the element, resisting the compressive forces at both joints resulting from pivoting of the hyomandibula during jaw protrusion. Further, these joints exhibit complex motion during prey capture and processing in *Narcine brasiliensis* and are the root of the unique asymmetrical jaw protrusion in this species (Dean and Motta, 2004a, b). Through unequal rotation of the proximal ends of the hyomandibulae, the jaws can be displaced laterally more than 60° from the animal's midline. The cranio-hyomandibular joint therefore behaves as a complex hinge with a diverse loading regime.

Functional Morphology of Trabeculation

There are two types of trabeculae in *Narcine brasiliensis*, each fulfilling a different function. In regions where loading is transverse and spatially restricted (e.g., the quadratomandibular joints, the hyomandibular-cranial joint, the depressor mandibularis attachment point), trabeculae are loaded in compression and lead the loads to the cortex on the opposite side of the lumen. These "load leading" trabeculae are also found in the durophagous myliobatid stingrays (see below). While a thick cortex serves to transmit forces only across the surface of the jaws, these trabeculae can dissipate loads from the occlusal surface through the lumen (Seilacher, 1979b; Sherrard, 2000).

The parasymphyseal trabeculae of *Narcine* perform a different function, acting as trusses to prevent buckling when the jaws are loaded axially (along the long-axis of the jaws) during jaw protrusion. While "load leading" trabeculae resist collapse in transverse loading, the parasymphyseal "truss" trabeculae are arranged perpendicular to load applied at the tips of the jaws. In this way, they act to preserve the distance between the lateral and medial rinds of the jaws (where the jaws are narrowest) and are therefore likely loaded in tension and compression. "Load leading" trabeculae are found in both *N. brasiliensis* and myliobatid rays; however, "truss" trabeculae are apparently a structural element unique to *N. brasiliensis*.

The excavation behavior of *Narcine brasiliensis* makes the "design" or constructional morphology of the parasymphyseal regions of the jaws an interesting problem. Although the parasymphyseal portions of the jaws contact the sediment first, they are comparatively slender. An end-loaded, narrow column (like the parasymphyseal region of the jaws) is in danger of buckling, as illustrated by attempts to slide the wrapper off a drinking straw by hitting its end on the table. The force required to cause Euler buckling in an end-loaded column is a function of the column's length (L), its elastic modulus (E), the second moment of area (I), and a coefficient of restraint (n), related to the way the column is fixed at the ends:

$$Force = [(n \times \pi^2 \times E \times I)/L^2] \quad (1)$$

The jaws of *Narcine* best approximate a column attached to a pin at one end in that their morphology constrains their motion in the parasagittal plane; the n -value for this arrangement is 1.0. If we consider the length and composition of the jaws to be fixed, manipulation of the second moment of area (the way material is organized around the neutral axis of the column) is the only way to increase the buckling threshold of the jaws. This can be accomplished by concentrating material at a distance from the neutral axis of the column (i.e., tesseræ) and along the axes of bending (i.e., trabeculae).

The longer a compressive element (e.g., the parasymphyseal regions of the jaws), the larger the second moment of area (I) needed to avoid Euler buckling with end-loading (Currey, 1984; Vincent and Owers, 1986). Second moment of area can be maximized geometrically by distributing material of the cross-sectional shape of the column to efficiently resist bending along specific axes (as in an I-beam). Therefore, a tube is stiff regardless of the axis of applied bending.

The parasymphyseal regions of both jaw elements are compressiform, ovular, and slightly c-shaped in cross-section, with the major axis oriented dorsoventrally and the concavity facing lingually. This departure from the theoretically ideal circular cross-section can be explained at two structural levels: the individual skeletal element, and the protruded jaw as a unit. The lateromedial axis of parasymphyseal cross-sections is much narrower than the dorsoventral axis, increasing the potential for buckling along the minor axis of each element. However, if the loading is transverse to the "c's" the additional material required to form a circular cross-section is extraneous. Corrugated roofs and Thomas Jefferson's serpentine walls are similar examples where c-shaped elements with adequate curvature resist deformation, even with limited wall thickness. Further, parasymphyseal trabeculae prevent the gross reductions in second moment of area that would occur were the two rinds to collapse into each other. This may indicate that trabeculae are better at maintaining second moment of area and resisting deformation than tesserae.

The cross-sectional shapes of the individual jaw elements also contribute to the strength of the protruded jaw as a unit. As the jaw protrudes, it folds in half at the symphyses (Fig. 1) such that the halves of each jaw (e.g., left and right sides of the palatoquadrate) come into contact at the midline. In this orientation, the c-shaped cross-sections of the four skeletal elements (both halves of the palatoquadrate and Meckel's cartilage) converge to form a circular cross-section for the protruded jaw complex, an ideal shape for efficient suction feeding. Cortical reinforcement along the major axis of each skeletal element may function to support points of contact in the interaction of skeletal elements.

Thickening the cortex and adding trabeculae are two methods of providing support for the loads experienced by the jaws. Trabeculae were only found in areas of high cortical thickness (Fig. 3), which were also the regions likely to experience the highest loads during feeding. This coupling of structural reinforcements may be a consequence of the cortex being constrained to a certain thickness. Several elasmobranchs have been shown to possess a consistent number of tesseral layers (Kemp and Westrin, 1979; Dingerkus et al., 1991b). If the number of tesseral layers in the cortex is developmentally constrained, trabeculae may be arranged in regions of

the jaws where the forces associated with feeding exceed the strength of these layers.

Phylogenetic Implications

Trabeculation has only been observed in one other group of elasmobranchs, the myliobatid stingrays. Summers (2000) examined cross-sections of jaws from the majority of batoid groups, as well as jaws from the holocephalan, *Hydrolagus colliei*. Myliobatid trabeculae are found in the parasymphyseal regions of the jaw arch and are also normal to the long axis of jaws (running dorsoventrally), but perpendicular to the lateromedial orientation of the parasymphyseal trabeculae of *Narcine brasiliensis*. Although both designs are apparently advantageous for resisting loading regimes experienced during feeding, this variation represents the functional difference between durophagous trabeculation and the type observed in *N. brasiliensis*. While the former is oriented to resist compressive forces associated with a diet of hard prey (i.e., "load leading" trabeculae), the latter prevents buckling in areas of dynamic axial loading (i.e., "truss" trabeculae). Further, myliobatid trabeculation is far denser and more robust than in any region of *N. brasiliensis* jaws (Dean, pers. obs.).

The phylogenetic placement of the Torpediniformes remains in question (Chu and Wen, 1979; Shirai, 1992; McEachran et al., 1996; Douady et al., 2002), although it is agreed that they are more basal than the Myliobatiformes. Dual occurrence of trabeculation indicates either independent derivation in both groups or secondary loss of trabeculation by the balance of the Batoidea (Fig. 5). The former is more parsimonious; therefore, trabeculation apparently arose to meet the functional demands associated with feeding modes that result in extreme loading environments. The presence of trabeculation, as well as gape-limiting jaw ligaments, in members of the Torpediniformes and Myliobatiformes lends some support to the phylogenies of Shirai (1992; Torpediniformes are the sister group to Rajiformes + Myliobatiformes) and Chu and Wen (1979; Rajiformes gave rise to Torpediniformes + Myliobatiformes), although additional studies are needed to further resolve the discrepancies between these phylogenies.

Functional adaptation has been examined far less in cartilage than in bone. Trabeculation and tesseration in cartilage provide important means of balancing rigidity and durability, thereby optimizing skeletal elements formed from tissue with apparently limited in vivo reorganization abilities (Moss, 1977; Myers and Mow, 1983). Many batoid groups remain to be examined for trabeculation, most notably the Pristiformes (sawfishes) and the other members of the Torpediniformes. While the narcinid (e.g., *Narcine*) and narkid (e.g., *Narke*) torpediniform rays primarily feed on soft-bodied invertebrates, the balance of the order is piscivorous (e.g., *Hypnos*, *Torpedo*).

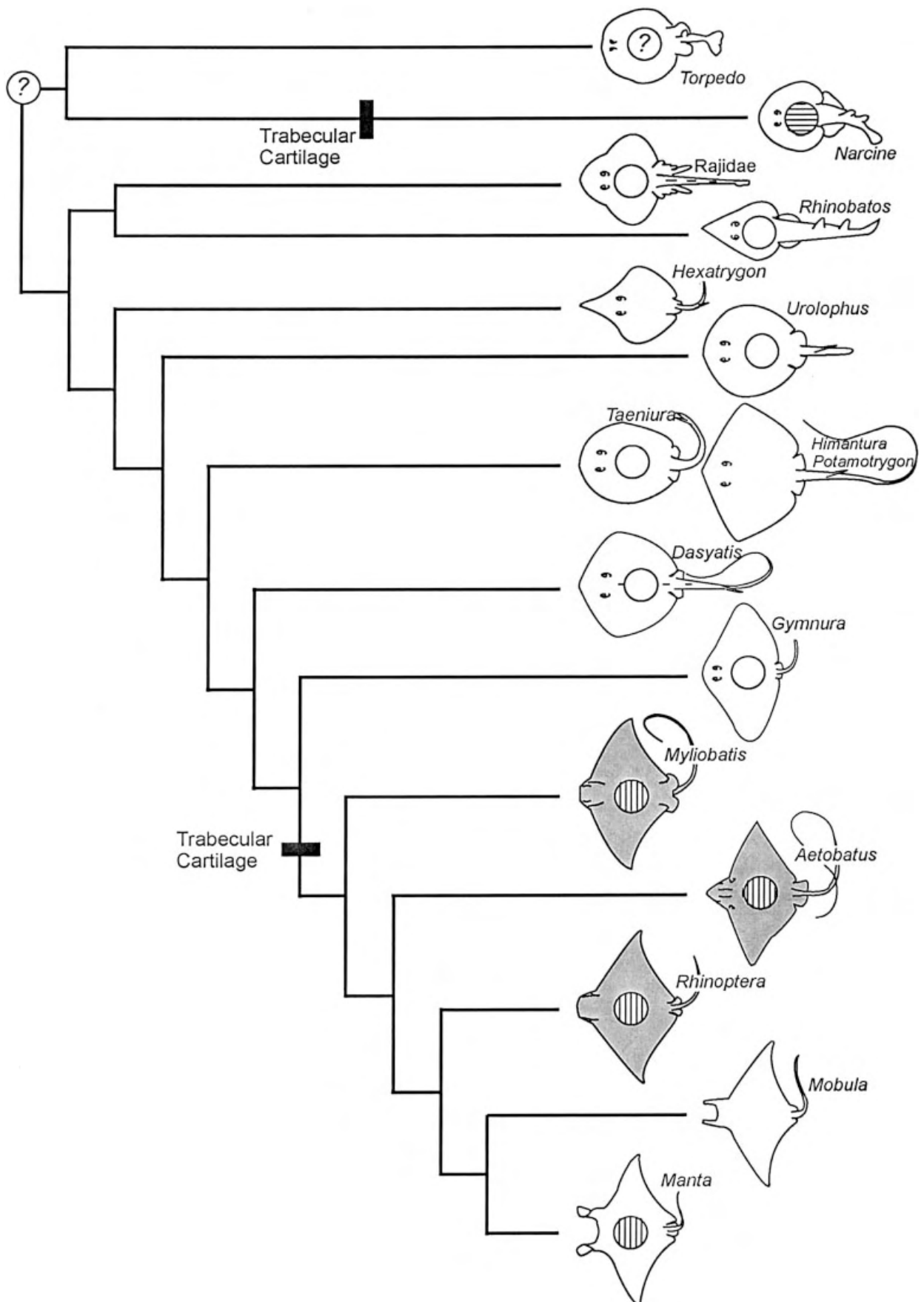


Fig. 5. Trabeculation in batoid elasmobranchs. Presence of trabecular cartilage is indicated by striped circles and durophagous genera are shaded. Trabeculae are found in the parasymphyseal region of the jaws in both *Narcine brasiliensis* and myliobatid rays. However, trabecular struts are arranged lateromedially in the former and dorsoventrally in the latter. The stripes inside of the circles are oriented perpendicularly to reflect this variation. Modified from Summers (2000), from a phylogeny by McEachran et al. (1996), with some groups omitted for clarity. Reprinted by permission of Wiley-Liss, Inc., a subsidiary of John Wiley & Sons, Inc.

The lack of trabeculation in the jaws of other piscivorous rays (*Gymnura*, *Dasyatis*; Summers, 2000) suggests that this method of structural support is restricted in the *Torpediniformes* to narcinid rays, with the particular arrangement likely derived in concert with the unique jaw protrusion mechanism.

CONCLUSIONS

The presence of trabeculation in the jaws and hyomandibulae of *Narcine brasiliensis* demands reevaluation of the evolution of these mineralized structures in Chondrichthyes. The occurrence of trabeculation in basal and derived Batoidea indicates two independent derivations of the structures, rather than the previously hypothesized single origin. Also, this first description of hyomandibular trabeculae illustrates that trabeculation is not a phenomenon restricted to jaw cartilage, but one that may be a phylogenetic response to extreme loads in all non-areolar calcified elasmobranch cartilage. A more extensive phylogenetic survey of elasmobranch cartilage is necessary.

“Load leading” trabeculae in *Narcine brasiliensis* serve a function similar to myliobatid trabeculae by transferring loads from restricted regions of the jaws through the lumen to the opposite cortex. “Truss” trabeculae, however, function to maintain an adequate second moment of area and represent a novel function for trabeculation in elasmobranchs.

ACKNOWLEDGMENTS

This work was graciously made more affordable by Matthew Colbert at UT Austin’s High Resolution CT Lab. George Burgess and Rob Robins donated specimens, as well as support and patience. John Currey was a meticulous editor and helped us develop the analogies of “truss” trabeculae and serpentine walls. Joe Bizzarro, Tom Koob, Phil Motta, Justin Schaefer, and Adam Summers provided valuable feedback and were constant sources of inspiration.

LITERATURE CITED

Bock WJ. 1964. Kinetics of the avian skull. *J Morphol* 114:1–42.
 Bock WJ. 1968. The avian mandible as a structural girder. *J Biomech* 1:89–96.
 Chu YT, Wen MC. 1979. Monograph of fishes of China (No. 2): a study of the lateral-line canals system and that of Lorenzini ampullae and tubules of elasmobranchiate fishes of China. Shanghai: Science and Technology Press.
 Currey JD. 1984. The mechanical adaptations of bones. Princeton, NJ: Princeton University Press.
 Currey JD. 2002. *Bones*. Princeton, NJ: Princeton University Press.
 Dean MN, Motta PJ. 2004a. Anatomy and functional morphology of the feeding apparatus of the lesser electric ray, *Narcine brasiliensis* (Elasmobranchii: Batoidea). *J Morphol* 262:462–483.
 Dean MN, Motta PJ. 2004b. Feeding behavior and kinematics of the lesser electric ray, *Narcine brasiliensis*. *Zoology* 107:171–189.
 Dingerkus G, Seret B, Guilbert E. 1991a. Multiple prismatic calcium phosphate layers in the jaws of present-day sharks (Chondrichthyes; Selachii). *Experientia* 47:38–40.

Dingerkus G, Séret B, Guilbert E. 1991b. Multiple prismatic calcium phosphate layers in the jaws of present-day sharks (Chondrichthyes; Selachii). *Experientia* 47:38–40.
 Douady CJ, Dosay M, Shivji MS, Stanhope MJ. 2002. Molecular phylogenetic evidence refuting the hypothesis of Batoidea (rays and skates) as derived sharks. *Mol Phylogenet Evol* 26:215–221.
 Herrel A, Aerts P, DeVree F. 1998. Ecomorphology of the lizard feeding apparatus: a modeling approach. *Neth J Zool* 48:1–25.
 Hylander WL, Johnson KR. 1997. In vivo bone strain patterns in the zygomatic arch of macaques and the significance of these patterns for functional interpretations of craniofacial form. *Am J Phys Anthropol* 102:203–232.
 Kemp NE, Westrin SK. 1979. Ultrastructure of calcified cartilage in the endoskeletal tesseræ of sharks. *J Morphol* 160:75–102.
 Ketcham RA, Carlson WD. 2001. Acquisition, optimization and interpretation of X-ray tomographic imagery: applications to the geosciences. *Comput Geosci* 27:381–400.
 Lanyon LE, Rubin CT. 1985. Functional adaptation in skeletal structures. In: Hildebrand M, Bramble DM, Liem KF, Wake DB, editors. *Functional vertebrate morphology*. Cambridge, MA: Harvard University Press. p 1–23.
 Martin RB, Burr DB, Sharkey NA. 1998. *Skeletal tissue mechanics*. New York: Springer.
 McEachran JD, Dunn KA, Miyake T. 1996. Interrelationships of the batoid fishes (Chondrichthyes: Batoidea). In: Stiassny MLJ, Parenti LR, Johnson GD, editors. *Interrelationships of fishes*. New York: Academic Press. p 63–84.
 Moss SA. 1977. Skeletal tissues in sharks. *Am Zool* 17:335–342.
 Myers ER, Mow VC. 1983. Biomechanics of cartilage and its response to biomechanical stimuli. In: Hall BK, editor. *Cartilage: structure, function and biochemistry*. New York: Academic Press. p 313–341.
 Olson WM. 2000. Phylogeny, ontogeny, and function: extraskeletal bones in the tendons and joints of *Hymenochirus boettgeri* (Amphibia: Anura: Pipidae). *Zoology* 103:15–24.
 Seilacher A. 1979a. Constructional morphology and evolutionary ecology of sand dollars. *Konstruktionsmorphologie* 157:169–172.
 Seilacher A. 1979b. Constructional morphology of sand dollars. *Paleobiology* 5:191–221.
 Sherrard KM. 2000. Cuttlebone morphology limits habitat depth in eleven species of *Sepia* (Cephalopoda: Sepiidae). *Biol Bull (Woods Hole)* 198:404–414.
 Shiller DM, Laboisière R, Ostry DJ. 2002. Relationships between jaw stiffness and kinematic variability in speech. *J Neurophysiol* 88:2329–2340.
 Shirai S. 1992. Squalean phylogeny: a new framework of “squaloid” sharks and related taxa. Sapporo: Hokkaido University Press.
 Summers AP. 2000. Stiffening the stingray skeleton — an investigation of durophagy in myliobatid stingrays (Chondrichthyes, Batoidea, Myliobatidae). *J Morphol* 243:113–126.
 Summers AP, Koob TJ, Brainerd EL. 1998. Stingrays jaws strut their stuff. *Nature* 395:450–451.
 Summers AP, Ketcham RA, Rowe T. 2004. Structure and function of the hornshark (*Heterodontus francisi*) cranium through ontogeny — the development of a hard prey specialist. *J Morphol* 260:1–12.
 Swartz SM, Parker A, Huo C. 1998. Theoretical and empirical scaling patterns and topological homology in bone trabeculae. *J Exp Biol* 201:573–590.
 Thomason JJ. 1995. To what extent can the mechanical environment of a bone be inferred from its internal architecture? In: Thomason JJ, editor. *Functional morphology in vertebrate paleontology*. Cambridge, UK: Cambridge University Press. p 249–263.
 Vincent JFV, Owers P. 1986. Mechanical design of hedgehog spines and porcupine quills. *J Zool (Lond)* 210:55–75.
 Wainwright SA, Biggs WD, Currey JD, Gosline JM. 1976. *Mechanical design in organisms*. Princeton, NJ: Princeton University Press.